The Effect of Prostaglandin Analogue Bimatoprost on Thyroid-Associated Orbitopathy

Catherine J. Choi,[1] Wensi Tao,[1] Ravi Doddapaneni,[1] Zenith Acosta-Torres,[1,2] Nathan W. Blessing,[1] Bradford W. Lee,[1] Daniel Pelaez,[1,2] and Sara T. Wester[1]

[1]Dr. Nasser Al-Rashid Orbital Vision Research Center, Bascom Palmer Eye Institute, Department of Ophthalmology, McKnight Vision Research Center, University of Miami School of Medicine, Miami, Florida, United States
[2]Department of Biomedical Engineering, University of Miami Miller School of Medicine, Miami, Florida, United States

Correspondence: Sara T. Wester, Department of Ophthalmology, Bascom Palmer Eye Institute, McKnight Vision Research Center, University of Miami School of Medicine, Room 804, 1638 NW 10th Avenue, Miami, FL 33136, USA; swester2@med.miami.edu.
Daniel Pelaez, Department of Ophthalmology, Bascom Palmer Eye Institute, McKnight Vision Research Center, University of Miami School of Medicine, Room 804, 1638 NW 10th Avenue, Miami, FL 33136, USA; dpelaez@med.miami.edu.

CJC and WT contributed equally to the work presented here and should therefore be regarded as equivalent authors.

Submitted: June 25, 2018
Accepted: November 2, 2018

Citation: Choi CJ, Tao W, Doddapaneni R, et al. The effect of prostaglandin analogue bimatoprost on thyroid-associated orbitopathy. *Invest Ophthalmol Vis Sci*. 2018;59:5912–5923. https://doi.org/10.1167/iovs.18-25134

Purpose. We characterize the effect of bimatoprost on orbital adipose tissue in thyroid-associated orbitopathy (TAO) with clinicopathologic correlation.

Methods. Orbital adipose-derived stem cells (OASCs) from types 1 and 2 TAO and control patients with and without exposure to 1 μm bimatoprost were examined via immunohistochemistry, RT-PCR, and Western blot for cell viability, migration capacity, lipid content, adipocyte morphology, mitochondrial content, and levels of adipogenic markers. A retrospective chart review was performed for clinicopathologic correlation. In mice, optical coherence tomography and pattern electroretinography were performed at baseline and at 1 month following a retrobulbar injection of bimatoprost, followed by orbital exenteration for histopathologic examination.

Results. Types 1 and 2 TAO-derived cells had a significantly higher migration capacity and lipid content than those of healthy controls. With the addition of bimatoprost, types 1 and 2 TAO and control adipocytes exhibited a significant decrease in lipid content with morphologic transformation into smaller and multilocular lipid droplets, and an increase in mitochondrial load and UCP-1 expression consistent with an increase in brown adipose tissue turnover. Retrobulbar injection of bimatoprost in mice did not alter the gross morphology, retinal thickness, or ganglion cell function in vivo.

Conclusions. Bimatoprost inhibits adipogenesis in OASCs and upregulates pathways involved in the browning of adipocytes. Furthermore, retrobulbar injection of bimatoprost is tolerated without immediate adverse effects in mice. Our results suggest a potential future application of prostaglandin analogues in the treatment of TAO.

Keywords: thyroid eye disease, bimatoprost, prostaglandins, adipogenesis, brown adipose tissue

Thyroid-associated orbitopathy (TAO), also called Graves' ophthalmopathy (GO), is an autoimmune disease that affects orbital adipose tissue and extraocular muscles.[1,2] Type 1 TAO typically is associated with expansion of the orbital adipose tissue, while type 2 TAO is characterized by extraocular muscle enlargement and fibrosis.[3] TAO can lead to an array of clinical manifestations, including proptosis, exposure keratopathy, restrictive strabismus, eyelid retraction, and compressive optic neuropathy.[4]

Examination of orbital tissue from TAO reveals increased deposition of glycosaminoglycans (GAG) within the endomysium of extraocular muscle fibers and increased de novo adipogenesis.[1–3] The main effector cell for GAG synthesis and adipogenesis is thought to be the orbital fibroblast (OF) with mesenchymal stem cell-like properties.[5] Thymocyte antigen 1-positive (Thy1+) OFs can differentiate into myofibroblasts with contractile properties when treated with TGF-β, while thymocyte antigen 1-negative (Thy1-) OFs differentiate into mature adipocytes when treated with PPARγ- agonists.[6] These OFs from TAO patients also have higher levels of expression of insulin-like growth factor 1 receptor (IGF1R), and in some instances, variably upregulated thyroid stimulating hormone receptor (TSHR) compared to controls.[7,8] TSHR antibodies acting upon upregulated IGF1R/TSHR functional complexes within the orbital tissue also are thought to lead to the downstream effects in OFs leading to TAO by potentiating PPARγ signaling.[8,9]

Currently available treatments for TAO include medical therapy for the treatment of hyperthyroidism and orbital inflammation, surgical therapy in the form of orbital decompression, eyelid surgery, strabismus surgery, and external beam orbital radiation.[4] These treatments show variable efficacy over a wide spectrum of disease severity, with a number of associated risks. Most recently, clinical trials for the human monoclonal antibody inhibitor of IGF1R, teprotumumab, have shown promise in the treatment of active TAO.[10] Additional studies and longer follow-up data, however, are needed to confirm these phase II study findings. An effective therapy targeting the complex pathogenic pathways of the underlying disease process remains elusive.

One such therapeutic candidate being proposed is bimatoprost. Bimatoprost is a prostaglandin F2 alpha (PGF2a) analogue used as topical therapy for glaucoma, which binds to a prostamide receptor composed of a heterodimer complex

Table. Clinical Summary

Diagnosis	Sex	Age	Thyroid Treatment	Smoking	Steroids	CON	CAS
Type 1	F	20	RAI, thyroidectomy	None	None	No	2/10
Type 1	F	57	Methimazole, thyroidectomy	None	None	No	5/10
Type 1	F	51	RAI	None	None	No	2/10
Type 2	F	55	RAI, thyroidectomy	35 pack-yrs, quit 3.5 yrs before CON	Oral	Yes	6/10
Type 2	F	74	RAI, thyroidectomy	None	Oral, IV	Yes	7/10
Type 2	F	55	RAI, thyroidectomy	Former (quit 1979, 0.5 pack years)	IV	Yes	NA
Type 2	F	65	Methimazole, thyroidectomy	Yes – ongoing smoker	Oral, IV	Yes	7/10
Control	M	77	NA	None	NA	NA	NA
Control	F	75	NA	None	NA	NA	NA
Control	F	60	NA	None	NA	NA	NA

F, female; M, male; RAI, radioactive iodine; CON, compressive optic neuropathy; IV, intravenous; CAS, clinical activity score; NA, not applicable.

of prostanoid F (FP) receptor and its splice variants.[11] In metabolically active tissue in vivo, bimatoprost also undergoes conversion into bimatoprost acid by tissue esterases, which then can bind the FP receptor itself and initiates a variety of intracellular signaling cascades.[11–13] Interestingly, long-term use of prostaglandin (PG) analogues has been shown to lead to PG-associated periorbitopathy (PAP), which is characterized by reversible atrophy of periorbital tissues, including orbital adipocytes.[14,15] While the molecular mechanism behind PAP remains incompletely elucidated, studies suggest that PG analogues, such as bimatoprost, decrease human preadipocyte differentiation and intracellular lipid accumulation by inhibiting the PPARγ pathway.[13,16]

The orbital fat atrophy associated with PAP has potential implications for type 1 TAO, in which abnormal orbital fat hypertrophy is seen. Harnessing the effect of PG analogues on adipogenic pathways to intentionally induce orbital fat atrophy in type 1 TAO has been proposed.[17] Biosynthesis of PG is dependent on the cyclooxygenase pathway, which in turn is intimately tied to white and brown adipose tissue physiology.[18] Adipose trans-differentiation, which previously has been studied in the context of metabolism, now also is thought to be involved in TAO adipose pathophysiology.[19] In murine models of TAO, studies have suggested white-to-brown adipose trans-differentiation with high levels of TSHR coexpression.[20,21]

To understand the adipogenic signaling pathways involved in PAP, and to study the potential efficacy of PG analogues in managing TAO, we used orbital adipose-derived stem cells (OASCs) from healthy controls and types 1 and 2 TAO patients as in vitro models of orbital adipose tissue physiology. Adipogenic potential of OASCs and the pathways downstream of the prostanoid FP receptor were studied with and without bimatoprost supplementation. Clinicopathologic correlation was made to identify any significant differences between types 1 and 2 TAO, and the implications behind the distinct clinical presentations and therapeutic applicability of PG analogues for each type. An additional in vivo safety study of retrobulbar injection of bimatoprost in mice also was performed. We believe our results suggested a potential future application of PG analogue physiology in the treatment of type 1 TAO.

Materials and Methods

Participants and Specimen Collection

Orbital fat tissues were harvested from TAO patients undergoing orbital decompression for either orbital rehabilitation or compressive optic neuropathy between 2015 and 2017 at the Bascom Palmer Eye Institute. Orbital fat from control patients was obtained during blepharoplasty procedures from medial upper eyelid or lower eyelid fat pads, which are contiguous with orbital fat and of the same embryonic lineage.[22] Patients with a prior history of orbital trauma, infection, surgery (excluding strabismus surgery), or orbital radiation were excluded. Three type 1 and four type 2 TAO patients, and three control patients were included in the study (Table). Medical records were reviewed for demographic information, history of medical and surgical treatments for thyroid disease, systemic corticosteroid therapy, and smoking. Clinical examination findings were reviewed and clinical activity scores (CAS) calculated for the seven patients with TAO. Collection and evaluation of protected patient health information were in compliance with the rules and regulations of the Health Insurance Portability and Accountability Act. Bascom Palmer Eye Institute and University of Miami Human Studies Committee completed an administrative review of the study and institutional review board approval was obtained. Informed consent was obtained from each participant for use of tissue for research purposes. All procedures performed in studies involving human participants were in accordance with the ethical standards of the institutional research committee and with the 1964 Declaration of Helsinki and its later amendments or comparable ethical standards.

OASC Isolation and Culture

OASCs were isolated as described previously from healthy controls and patients with TAO.[23,24] Orbital fat tissue was cut into sections <5 mm in size. Adipose tissue was subjected to digestion with 1 mg/mL Col I (Worthington Biochemical Corp, Lakewood, NJ, USA) in Dulbecco's modified Eagle's medium (DMEM) for 3 hours on a shaker. Digested tissue was pipetted up and down 10 times before centrifugation at 300*g* for 5 minutes to remove floating adipocytes. The pellets were suspended in DMEM and filtered through a 70 μm nylon strainer (BD Bioscience, Franklin Lakes, NJ, USA) to yield cells in the flow-through as stromal vascular fraction (SVF). Cells in SVF were treated with red blood cell lysis buffer to remove red blood cells and with 0.25% trypsin-EDTA for 5 minutes at 37°C to yield a single cell suspension. Cells were maintained in DMEM containing 10% fetal bovine serum (FBS) at 37°C with 5% CO_2.

Cell Viability Assay

OASCs from healthy controls were seeded at a density of 5×10^3 cells/well in 96-well plates in 100 μL media. After 24 hours, OASCs were treated with bimatoprost (0.25–10 μM) (Selleckchem Catalog No.S1407; Selleckchem, Houston, TX, USA) for 72 hours. After treatment, 3-(4, 5-dimethylthiazol- 2-yl)-2, 5-diphenyltetrazolium bromide (MTT) assay (Biotium, Fremont, CA, USA) was performed according to the manufacturer's

instructions to measure the mitochondrial metabolism rate as a surrogate indicator for proliferation and viability. Briefly, MTT (5 mg/mL) was added and plates were incubated at 37°C for 4 hours before dimethyl sulfoxide (DMSO; 100 μL) was added to each well. Finally, the absorbance of each well was read at a wavelength of 570 nm using a scanning multiwell spectrophotometer. The results were analyzed using statistical methods in three independent experiments.

Cell Migration Assay

Cell migration was measured by the scratch wound healing assay. After reaching confluence, OASCs from TAO and healthy control patients were pretreated with bimatoprost (1 μM) or DMSO for 3 hours. A wound then was introduced in the monolayer of cells by scratching with a p200 pipette tip. Images of an individual spot were captured at the time of scratch and at regular intervals (15 minutes) during cell migration with an inverted Zeiss Axio Observer Z1 microscope for 24 hours. Time-lapse videos were generated by microscope software AxioVision (Carl Zeiss Meditec, Jena, Germany). Average migration distance was measured and quantified with AxioVision software.

Adipogenesis Assay

OASCs during passages three to five were seeded at a density of 2.5×10^4 cells per cm^2 in 24-well PL plates in DMEM with 10% FBS. At 90% confluence on day 3, the medium was switched to the Adipogenesis Differentiation Medium (Invitrogen, Carlsbad, CA, USA). Bimatoprost (1 μM; Selleckchem Catalog No.S1407) was added on day 6 after differentiation of OASC into mature adipocytes. After 21 days of culturing, the cells were fixed with 4% paraformaldehyde (PFA) and stained with oil red O for adipocytes from the Adipogenesis Assay Kit (Cayman Chemical Company, Ann Arbor, MI, USA) according to the manufacturer's protocol. Cells with oil droplets stained by oil red O were quantified via spectrophotometry at an absorbance of OD 492 nm in triplicate cultures.

Immunohistochemistry

Before immunostaining, OASCs were fixed in 4% PFA for 12 minutes and permeabilized in 0.3% Triton X-100 in PBS for 30 minutes. Cells were blocked with PBS containing 0.15% Tween 20, 2% BSA, and 5% serum at room temperature for 30 minutes. The samples then were incubated with primary antibodies for 16 hours in blocking solution, followed by species-specific secondary antibodies (AlexaFluor; Thermo Fisher Scientific, Waltham, MA, USA). Control samples were incubated without primary antibodies. Neutral lipid was labeled by 4,4-difluoro-3a,4adiaza-s-indacene (BODIPY) dye and nucleic acids with 4′,6-diamidino-2-phenylindole (DAPI). Imaging was performed with a Leica TSL AOBS SP5 confocal microscope (Leica Microsystems, Exton, PA, USA). Confocal settings (laser intensity, detector gain, and pinhole size) remained constant among different groups.

Quantitative Real-Time (RT) PCR

Quantitative RT-PCR analysis was performed as described previously using gene-specific primers: PPAR-γ (5′ GATA CACTGTCTGCAAACATATCACAA 3′ CCACGGAGCTGATCC CAA), Human β-actin (5′ CACCAACTGGGACGACAT 3′ ACAGCCTGGATAGCAACG) UCP-1 (5′ CCACTTGGTGTCG GCTCTTA 3′ GTTCCAGGATCCAAGTCGCA), and PGC1-α (5′ CAGGTGCCTTCAGTTCACTCT 3′ GGTCTTCACCAACCAGA GCA). Relative expression was calculated using the standard curve method and normalized to housekeeping gene β-actin.

Western Blot Analysis

OASCs were lysed with T-PER buffer (Thermo Fisher Scientific) supplemented with complete protease inhibitor (Roche Applied Science, Indianapolis, IN, USA). An equal amount of total protein from each sample was resolved on SDS-PAGE gradient gels and transferred to a polyvinylidene difluoride (PVDF) membrane (Thermo Fisher Scientific). The membranes were blocked in 5% skim milk in Tris-buffered saline (TBS; pH 7.6), probed overnight with primary antibodies (UCP1, PPAR-γ, Phospho-Akt, Phospho-p44/42 MAPK, Erk1/2, Phospho-p38 MAPK – rabbit [Cell Signaling, Danvers, MA, USA]; PGC-1α, anti-mitochondria – rabbit [Abcam, Cambridge, UK]; and B-actin – mouse [Sigma-Aldrich Corp., St. Louis, MO, USA]), washed in 0.15% Tween20 in TBS, and incubated for 1 hour with a secondary antibody (1:10,000; GE Healthcare Bio-Sciences, Pittsburgh, PA, USA) diluted in TBS. Anti-β-actin antibody was used as the loading control. Proteins were visualized using SuperSignal chemiluminescent substrates (Thermo Fisher Scientific).

Calcium Imaging

Changes in the intracellular calcium levels were measured by the Fluo-4 Calcium Imaging Kit (F10489; Molecular Probes, Eugene, OR, USA). Time-lapse videos of 120 seconds were generated for OASCs from healthy patients with and without 1 μM bimatoprost treatment for 3 hours. Intensities of individual OASCs were quantified ($n = 25$) for treated and untreated cells and plotted as average change in intensity of fluorescence.

Retrobulbar Injection of Bimatoprost

To test the effects of bimatoprost in vivo, 100 μL 0.03% bimatoprost ophthalmic solution LATISSE was administered via retrobulbar injection in eight mice. PBS was injected in the contralateral orbit as control. Retinal nerve fiber layer (RNFL) thickness was measured by optical coherence tomography (OCT) at baseline before and at 1 month after injection. Pattern electroretinography (PERG) also was performed at baseline and at 1 month after injection to demonstrate retinal ganglion cell (RGC) function. The orbits subsequently were exenterated for histopathologic examination. All experiments were conducted in accordance with the Association for Research in Vision and Ophthalmology (ARVO) Statement for the Use of Animals in Ophthalmic and Visual Research. The experimental protocol was approved by the Institutional Animal Care and Use Committee at the University of Miami.

Statistical Analysis

Statistical analyses were performed using SAS Studio university edition (SAS Institute, Cary, NC, USA) and Graph Pad Prism 7 (GraphPad Software, La Jolla, CA, USA). Statistical analyses were performed with 2-tailed Student's *t*-tests and 1-way ANOVA with a confidence level greater than 95%. $P < 0.05$ was deemed statistically significant. Graphic data are presented as mean ± SEM.

Results

Effect of Bimatoprost on Cell Viability and Migration

A possible role for the PG pathway in TAO was demonstrated previously via RNA sequencing of OASCs from patients with

Investigative Ophthalmology & Visual Science

TAO and healthy controls, where differential expression of PG receptors was noted between the two groups (Fig. 1A). Therefore, we first explored the viability and migration of OASCs after bimatoprost treatment; 2 and 10 μM bimatoprost significantly inhibited the cell viability of OASCs derived from healthy control patients ($P = 0.005$ and $P = 0.035$), while the effect of 1 and 0.25 μM bimatoprost was within the margin of error (1 μM, $P = 0.3325$; 0.25 μM, $P = 0.4872$; Fig. 1B). At day 7, cell viability of OASCs from types 1 and 2 TAO patients was significantly higher than that of control (type 1, 152.7%, $P = 0.0279$; type 2, 193.6%, $P = 0.0143$). Addition of 1 μM bimatoprost inhibited the cell viability of control, and types 1 and 2 TAO OASCs at day 7 (control, $P = 0.0513$; type 1, $P = 0.0322$; type 2, $P = 0.0126$; Fig. 1C).

In terms of cell migration, OASCs derived from types 1 and 2 TAO patients demonstrated a higher migration capacity than control OASCs at baseline (type 1, 119.5%, $P = 0.0132$; type 2, 127.2%; $P = 0.0242$). One μM bimatoprost inhibited cell migration in OASCs from TAO and control patients (Fig. 1D). Bimatoprost treatment significantly reduced the migration distance of OASCs derived from type 1 TAO patients from 119.5% ± 6.51 to 108.6% ± 3.05 ($P = 0.0419$), type 2 TAO patients from 127.2% ± 4.78 to 108.7% ± 4.56 ($P = 0.0231$) and control patients from 100% ± 3.54 to 81.23% ± 5.41 ($P = 0.0409$) within 24 hours (Fig. 1E).

Bimatoprost Inhibits the Adipogenic Capacity of OASCs

OASCs from healthy control and TAO patients were differentiated into adipocytes with and without bimatoprost in the culture medium (1 μM; Fig. 2A). Quantification of lipid content as a measure of adipogenic capacity revealed higher baseline neutral lipid content in adipocytes from types 1 ($P = 0.0214$) and 2 ($P = 0.0348$) TAO patients compared to those from healthy patients (Figs. 2B, 2C). Furthermore, type 1 TAO adipocytes exhibited higher lipid content than type 2 TAO adipocytes ($P = 0.0419$). Bimatoprost then was shown to inhibit adipogenesis in adipocytes from types 1 ($P = 0.0162$) and 2 ($P = 0.0259$) TAO and healthy ($P = 0.0319$) patients. In terms of cell morphology, bimatoprost-treated adipocytes from TAO and healthy patients demonstrated smaller multilocular lipid droplets compared to untreated cells containing larger, unilocular lipid droplets (Fig. 2B). This formation of multilocular lipid droplets is consistent with possible white-to-brown adipose trans-differentiation.

Bimatoprost Promotes Browning of Differentiated Adipocytes Through Mitochondrial Biogenesis

Increased mitochondrial contents are the hallmark of browning of white adipocytes. Using epifluorescence microscopy, we demonstrated an increased MitoTracker staining with bimatoprost treatment in differentiated adipocytes derived from TAO and healthy patient OASCs (Fig. 3A). The increased mitochondrial staining was detected only in differentiated adipocytes and not in the undifferentiated fibroblasts. Furthermore, in OASCs from types 1 and 2 TAO and control patients, bimatoprost increased the expression of brown adipocyte marker UCP-1 and mitochondrial biogenesis marker PGC-1α, while levels of adipogenesis marker PPAR-γ remained similar before and after treatment (Fig. 3B). RT-PCR also showed consistent results at the level of mRNA expression of the three markers (Fig. 3C). Immunofluorescence stain in OASCs for neutral lipids and UCP-1 also demonstrated concurrent formation of multiple small multilocular lipid droplets and increased expression of UCP-1 in response to bimatoprost (Fig. 3D). These findings together suggest that bimatoprost has a role in stimulating white-to-brown adipose trans-differentiation via mitochondrial biogenesis.

Bimatoprost Activates MAPK, PI3/Akt, p38 MAPK, and Calcium Signaling Pathways

We assayed the protein levels of the phosphorylated forms of ERK, Akt, and p38 by Western blot. In OASCs from TAO and healthy patients, bimatoprost appeared to activate these signaling pathways as demonstrated by upregulation of their respective phosphorylation products (Fig. 4A). To further study the potential role of these pathways, MEK inhibitor U0216, Akt inhibitor MK-2206, and p38 inhibitor SB202190 then were added to the OASC cultures along with bimatoprost (Fig. 4B). Following adipocytic differentiation, all three inhibitors were noted to partially rescue the inhibitory effect of bimatoprost on adipogenesis as demonstrated by oil red O staining and measurement of neutral lipid content ($P = 0.0232$, 0.0342, 0.0198; Figs. 4C, 4D). Lastly, a role for calcium signaling with bimatoprost was shown in OASCs from healthy control patients where the fluorescence intensity corresponding to intracellular calcium levels increased for 120 seconds with the addition of bimatoprost (Figs. 4E, 4F).

Retrobulbar Injection of Bimatoprost Does Not Lead to Histologic or Functional Changes

Hematoxylin and eosin (H&E)–stained sections of orbits treated with retrobulbar injection of bimatoprost showed normal morphology of ocular and orbital structures (Fig. 5A). The RNFL thickness remained unchanged (bimatoprost 58.50 ± 7.219 μm vs. PBS 56.75 ± 6.421 μm; $P = 0.3837$; Figs. 5B, 5C) and PERG amplitudes before and after treatment in PBS control and bimatoprost-treated eyes did not show any statistically significant differences (baseline, 19.93 ± 2.854 μV vs. post-bimatoprost treatment 18.67 ± 2.311 μV, $P = 0.5618$; baseline 19.13 ± 2.292 μV vs. post-PBS 18.27 ± 3.031 μV, $P = 0.4317$; Figs. 5D–F). The PERG peaks and waveforms also were very similar between the bimatoprost-treated and control eyes (Figs. 5D–F).

Discussion

TAO is an autoimmune disease most commonly associated with Graves' disease, but also seen in patients with hypothyroidism, chronic autoimmune thyroiditis, or in some cases, euthyroidism. Annual incidence is estimated to be 16 per 100,000 in women and 2.9 per 100,000 in men.[25] The major pathologic features include expansion of orbital soft tissues and enlargement of extraocular muscles. Type 1 TAO is characterized by increased orbital adipogenesis, in which multipotent orbital fibroblasts differentiate into mature adipocytes via PPARγ signaling. There is an overexpression of PPARγ in the adipose tissue of active TAO, and PPARγ agonists also have been shown to increase TSHR expression, further potentiating this pathway.[26–29]

At the other end of the spectrum, PAP is a known side effect of topical PG analogues used to treat glaucoma. PAP is characterized by periorbital lipodystrophy leading to enophthalmos and superior sulcus deformity.[30] Activation of the prostanoid FP receptor by a PGF2α analogue has been shown to lead to inhibition of PPARγ.[31] PGF2α significantly reduces proliferation and adipogenesis in murine preadipocytes and human orbital fibroblasts, while the rate of lipolysis remains unaffected.[17,32,33] Furthermore, our previous study into the gene expression profiling of OASCs from TAO and control

Investigative Ophthalmology & Visual Science

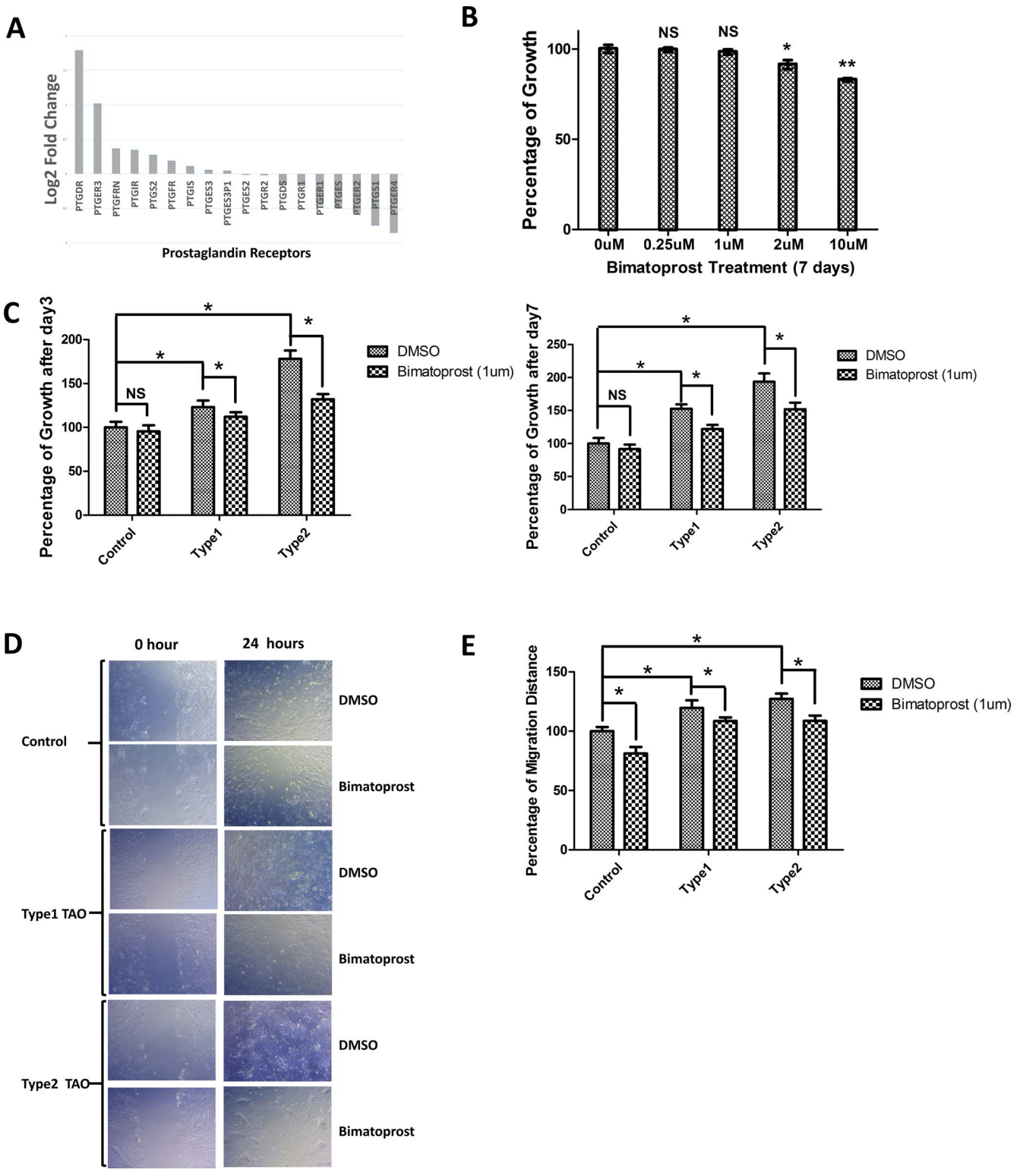

Figure 1. Differential expression of PG receptors in TAO and the effect of bimatoprost on cell viability and migration. (**A**) RNA-sequencing analysis of OASCs from TAO patients compared to control patients demonstrating differential expression of PG receptors identified by EdgeR and DESeq2. (**B**) Dose-dependent cell viability of OASCs from healthy controls treated with bimatoprost. (**C**) Cell proliferation of OASCs from healthy controls, and types 1 and 2 TAO patients treated with bimatoprost on days 3 and 7. (**D**) Scratch assay showing the effect of 1 μM bimatoprost on OASC migration over a 24-hour period. (**E**) Quantification of 24-hour migration data in control and TAO OASCs. $^{*}P < 0.05$, $^{**}P < 0.01$. NS, not significant. *Scale bar*: 200 μm.

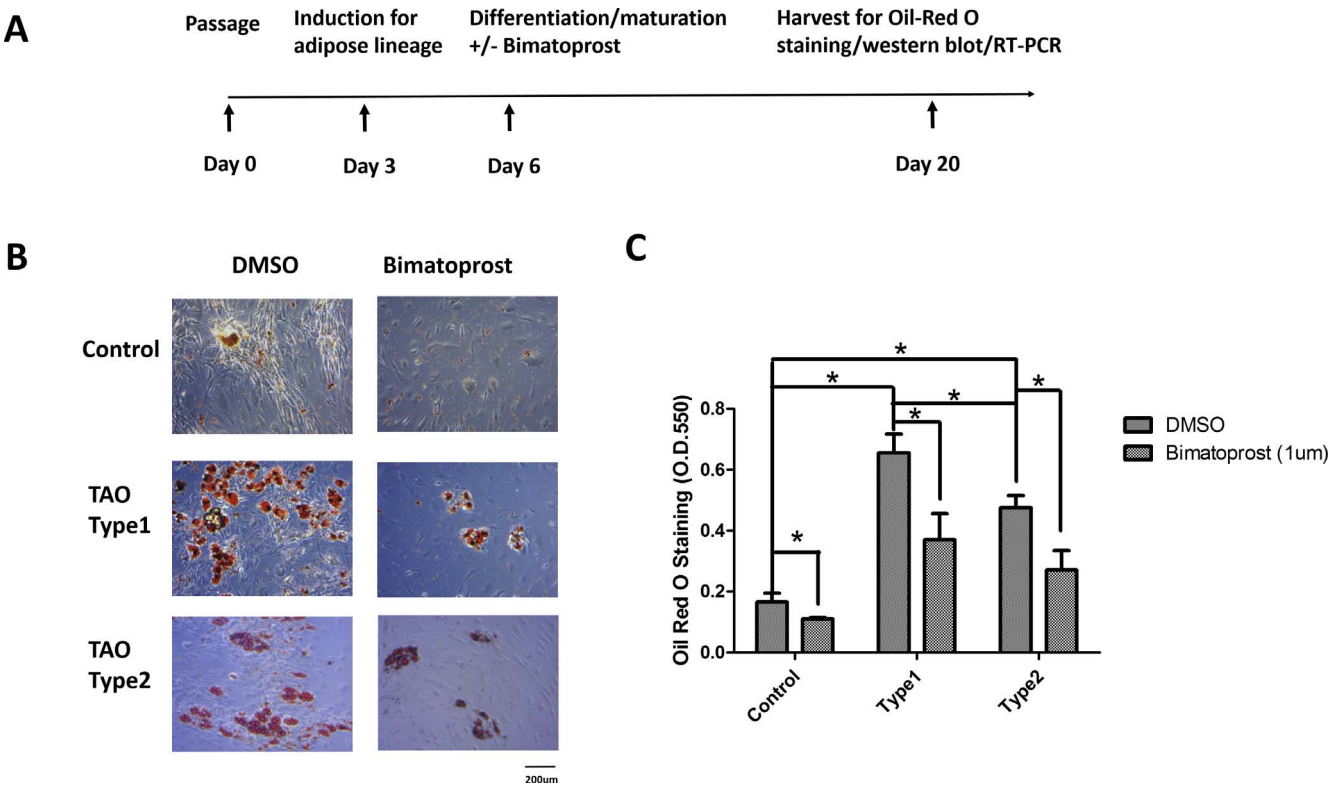

Figure 2. Bimatoprost inhibits OASC adipogenesis. (**A**) A timeline of the adipogenesis assay. (**B**) Oil red O stain demonstrating bimatoprost-treated adipocytes with smaller, multilocular lipid droplets compared to vehicle-treated cells containing larger, unilocular lipid droplets. (**C**) Quantification of oil red O assay showing higher baseline neutral lipid content in type 1 > type 2 TAO adipocytes compared to control, and inhibition of adipogenesis in control and TAO OASCs with bimatoprost. $^{*}P < 0.05$, $^{**}P < 0.01$. *Scale bar*: 200 µm.

patients revealed several PG receptors as differentially expressed and upregulated in TAO-derived stem cells (Fig. 1A).

Thus, type 1 TAO demonstrates increased orbital adipogenesis and dysregulation of PG receptor expression, whereas PAP is characterized by periorbital fat atrophy via potentially overlapping molecular pathways. Given these two seemingly inversely related phenomena, we hypothesized that using the PG analogue's ability to induce orbital fat atrophy may have potential implications for the clinical management of type 1 TAO. Therefore, our purpose was to elucidate these overlapping signaling pathways in PAP and TAO in vitro and in vivo, and correlate with clinical presentation via a number of proof-of-concept experiments.

To this end, OASCs from healthy controls and types 1 and 2 TAO patients were used as in vitro models of orbital adipose tissue, and bimatoprost was chosen as the representative PG analogue based on previous data demonstrating its high potency and efficacy in inducing PAP among various PG analogues.[8,10] Representative and comparable age groups were chosen for controls and TAO patients. The appropriate concentration of bimatoprost to be used was first titrated with a cell viability assay in OASCs from healthy controls (Fig. 1B). One µM was shown to be the highest concentration tolerated by OASCs without affecting cell viability, and, thus, chosen as the standard concentration for all subsequent bimatoprost treatments.

An important baseline difference between OASCs from healthy controls and TAO patients was demonstrated by the cell growth (Fig. 1C) and wound healing assay (Figs. 1D, 1E). OASCs from types 1 and 2 TAO showed increased cell viability at days 3 and 7 compared to controls, suggesting that the increased orbital fat proliferation in TAO may be secondary to adipose cell survivability and longevity, as well as decreased apoptosis. It also should be noted that the assay may reflect the higher metabolic rate of TAO OASCs as measured by the catabolism of tetrazolium salts. OASCs from types 1 and 2 TAO also had a significantly higher migration capacity than those of healthy controls, suggesting that these cells are more likely to infiltrate into the target tissues during the inflammatory response of TAO. With the addition of bimatoprost, there was a significant decrease in viability and migration of TAO OASCs, constituting a generalized inhibitory effect.

The adipogenesis assays were consistent with the clinical picture of TAO in that TAO cells demonstrated significantly higher total lipid content compared to controls, and this effect was accentuated in type 1 more so than type 2 TAO. Interestingly, the addition of bimatoprost led to a decrease in lipid content in control and types 1 and 2 TAO adipocytes. This effect was most dramatic, however, in type 1 TAO as was hypothesized. The results in type 2 TAO cells suggested that while the predominant clinical changes in type 2 TAO are with extraocular muscle enlargement, there is some concurrent involvement of the orbital fat compartment, which can be targeted by bimatoprost.

The cell migration and adipogenesis assays together suggest that OASCs can, in fact, be used as a reliable in vitro model for TAO in that the cellular characteristics of increased proliferative and adipogenic capacity are consistent with the clinical manifestations of TAO. Furthermore, the inhibitory effect of bimatoprost on OASCs and differentiated adipocytes supports the hypothesis as it relates to PAP.

The phenotypic changes of adipocytes noted in the adipogenesis assay, on the other hand, suggest a possible role of white-to-brown adipose trans-differentiation in TAO and its

Investigative Ophthalmology & Visual Science

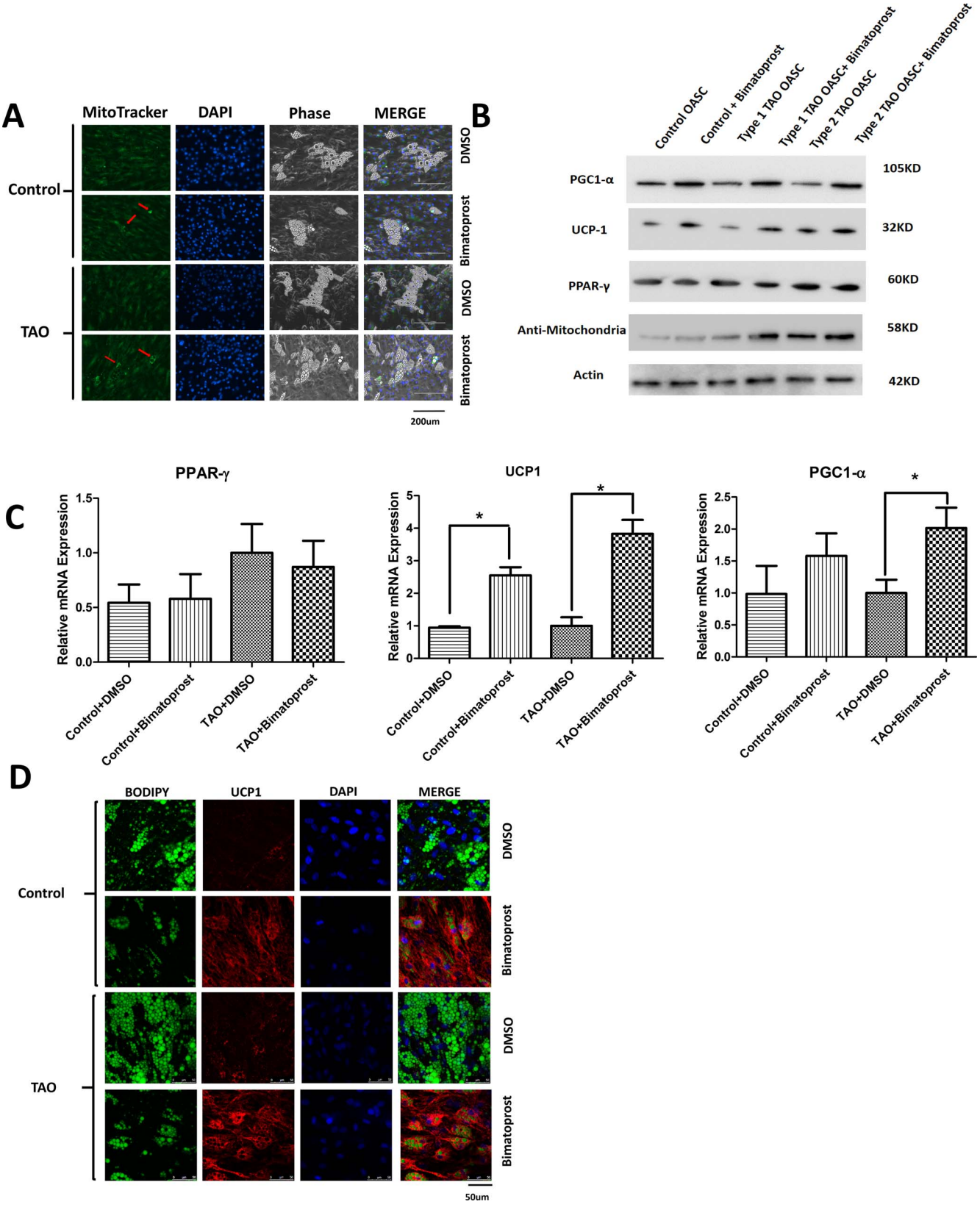

Figure 3. Bimatoprost induces mitochondrial biogenesis and triggers white-to-brown adipose trans-differentiation. (**A**) Mitochondrial content labeled with MitoTracker (*green*) and nuclear counterstaining with DAPI (*blue*) showing increased mitochondrial contents in adipocytes treated with bimatoprost (*arrows*). (**B**) Western blot analysis and (**C**) RT-PCR demonstrating increased expression of UCP-1 and PGC-1α with bimatoprost treatment, while PPAR-γ remained unchanged. (**D**) Immunofluorescence staining demonstrating formation of multiple small multilocular lipid droplets and increased expression of UCP-1 in response to bimatoprost treatment. $^{*}P < 0.05$. *Scale bars*: (**A**) 200 μm; (**D**) 100 μm.

Investigative Ophthalmology & Visual Science

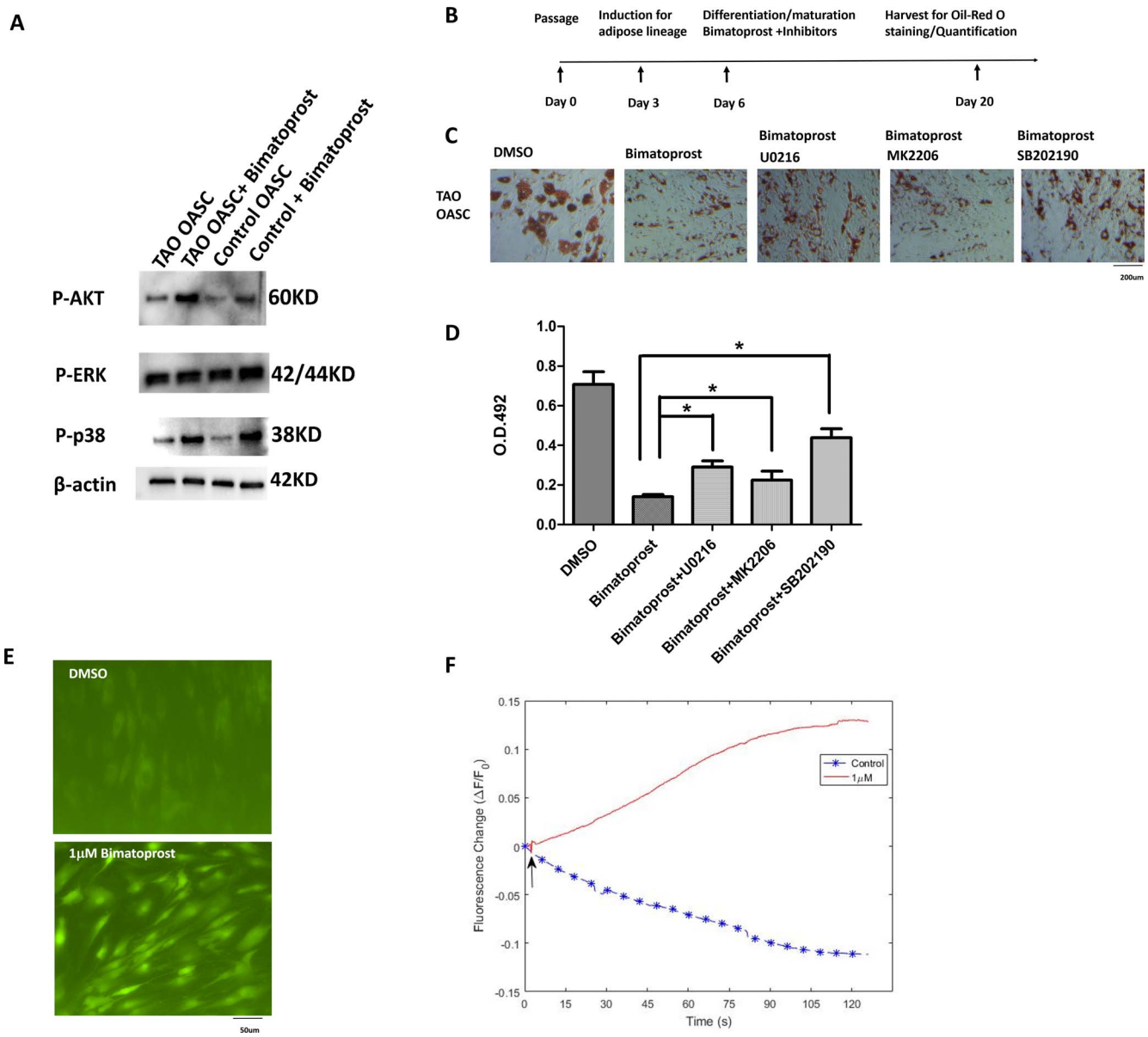

FIGURE 4. MAPK and Akt signaling pathways are activated by bimatoprost. (**A**) Western blot analysis demonstrating upregulation of phosphorylated ERK1/2, Akt, and p38 in response to bimatoprost treatment. (**B**) Schematic timeline of the adipogenic differentiation protocol. MEK inhibitor U0216, AKT inhibitor MK-2206, or p38 inhibitor SB202190 was added concurrently with bimatoprost after adipocyte lineage induction. (**C**) Oil red O staining and (**D**) quantification showing partial rescue from the inhibitory effect of bimatoprost on adipogenesis by all three inhibitors. (**E**) Fluorescent images and quantification (**F**) of intracellular transient calcium flux induced by bimatoprost treatment in OASCs. *Arrow* indicates time point of 1 μM bimatoprost addition. Data depicted as mean ± 95% confidence interval for $n = 25$ cells. *$P < 0.05$. *Scale bar*: 200 μm.

complex interrelationship with the effect of bimatoprost on adipose physiology. White adipose cells are large spherical cells with 90% of their cytoplasmic volume occupied by a unilocular lipid droplet filled with triglycerides, whereas brown adipose cells are packed with a higher concentration of spherical mitochondria with dense cristae and multilocular droplets of triglycerides.[27] The primary function of white adipose tissue (WAT) is energy storage in the form of lipids, while brown adipose tissue (BAT) dissipates energy in the form of heat for thermoregulation.[34] Depots of WAT and BAT exist in different areas of the body and their trans-differentiation has been studied extensively in the context of metabolism.[19] The trans-differentiation also is thought to determine the extent of macrophage infiltration and resultant chronic low-grade inflammation within the adipose tissue throughout the body.[32] WAT and BAT physiology and their implications in TAO were highlighted in a murine model of TAO created via electroporation of plasmid encoding human TSHR A-subunit.[20,21] Orbital adipogenesis in this murine TAO model demonstrated increased BAT marker UCP-1, while the total amount of orbital adipose tissue remained stable, implying a white-to-brown adipose trans-differentiation with development of TAO.[20] The investigators also noted high levels of coexpression of TSHR in UCP-1–positive BAT and hypothesized that the role of TSHR as the target antigen of TAO further supports the relative increase of BAT in TAO.[20]

In our study, addition of the PG pathway to the WAT and BAT physiology, however, resulted in a more complex picture. Activation of the adrenergic pathway within WAT leads to cyclooxygenase-2-mediated PG synthesis and browning of

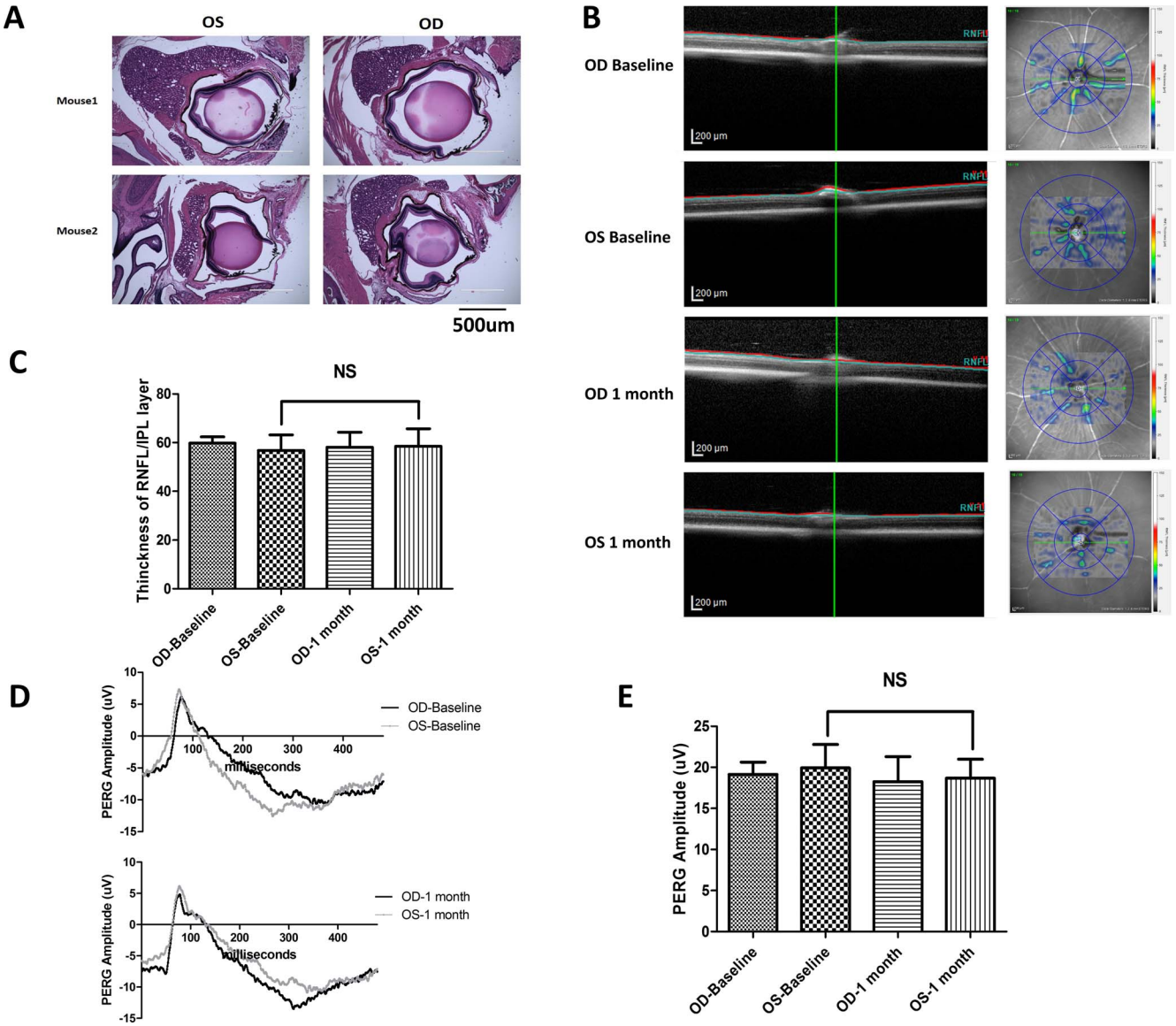

Figure 5. Gross morphology and histology of orbital tissues, retinal layer thickness, and RGC function after retrobulbar injection of bimatoprost. (**A**) H&E sections showing normal gross morphology of the orbit and surrounding orbital tissue in the bimatoprost-treated eyes (OS) and PBS-treated eyes (OD). (**B**) Representative images of OCT and fundus auto fluorescence (FAF) overlaid with retinal thickness heat maps generated by Heidelberg retina tomography. (**C**) RNFL thickness quantification showing no difference between bimatoprost-treated eyes (OS) and PBS-treated eyes (OD) at 1 month. (**D**) Representative PERG amplitudes waveforms showing no significant differences between bimatoprost- and PBS-treated eyes at baseline, and at 1 month after treatment. (**E**) Quantitative representation of PERG amplitude recordings in PBS- and bimatoprost treated eyes. NS, not significant. *Scale bars*: (**A**) 500 µm; (**B**) 200 µm.

WAT.[18] This PG-mediated white-to-brown trans-differentiation was, in fact, demonstrated in our study by mitochondrial biogenesis assays in adipocytes from TAO and healthy control patients. As highly metabolically active, thermogenic tissue, BAT has a number of key components in its molecular machinery. Uncoupling protein-1 (UCP-1), located in the inner membrane of mitochondria in BAT, decreases the transmembrane proton gradient and "uncouples" the oxidative phosphorylation resulting in dissipation of energy as heat. PPARγ is a nuclear receptor that functions as a key transcription factor in adipogenesis, and PGC-1 is a cofactor of PPARγ that induces UCP-1 expression. Therefore, measure of mitochondrial contents, and levels of UCP-1, PPARγ, and PGC-1 expression can be used to characterize the adipose tissue. In adipocytes derived from TAO and healthy control patients, bimatoprost treatment led to an increase in mitochondrial contents and UCP-1 levels consistent with increase in BAT (Figs. 3A–D). PGC-1 expression level showed a significant increase in TAO adipocytes only, and a trend toward an increase in healthy control adipocytes, while PPARγ levels remained unchanged for both types (Figs. 3B, 3C). These results appear to be consistent with white-to-brown trans-differentiation with bimatoprost in that brown adipose markers are upregulated without concurrent increase in de novo adipogenesis via the PPARγ pathway.

Reconciling the findings from previous studies suggesting white-to-brown adipose trans-differentiation in the development of TAO with bimatoprost-induced white-to-brown adipose trans-differentiation is challenging. When the effect of bimatoprost is being considered as potential therapy for TAO, it is paradoxical to suggest that TAO develops with the very same underlying process. It is interesting to note, however, that in

Investigative Ophthalmology & Visual Science

the murine models of TAO, orbital inflammation was limited to extraocular muscles and optic nerve without involving the adipose tissue.[21] Therefore, it is likely that the findings of this murine TAO model are not entirely representative of the full spectrum of TAO phenotypes, and perhaps are closer to type 2, rather than type 1 TAO. Additional studies are warranted to further elucidate the role of WAT and BAT in TAO.

To elucidate potential pathways by which bimatoprost may be exerting its effect on adipose tissue, a number of other key signaling pathways involved in adipogenesis also were examined. Bimatoprost is a prodrug, in which the C-terminal is methyl-esterified. In vivo, tissue esterase can degrade bimatoprost into bimatoprost acid, which then binds the prostanoid FP receptor.[11] Previous studies have demonstrated that activation of the prostanoid FP receptor by bimatoprost turns on the PI3K/Akt and MAPK/ERK pathways in murine myoblasts and retinal ganglion cells, respectively.[20] In feline iris sphincter cells, bimatoprost has been noted to selectively stimulate the p38 MAPK pathway, as well as intracellular calcium signaling.[22,23] MAPK/ERK, PI3K/Akt, and p38 MAPK also are each known to lead to variable activation and inhibition of PPARγ and its interactors. MAPK/ERK is thought to phosphorylate another adipogenic transcription factor, C/EBPβ, to activate PPARγ during the expansion phase of adipogenesis, then inhibits the transcriptional activities of PPARγ by phosphorylation in the terminal phases of adipocyte differentiation.[35,36] P38 MAPK can phosphorylate to inhibit a nuclear transcriptional factor NFAT, which in turn activates PPARγ.[37] These pathways also have been shown to be intricately linked to the WAT and BAT physiology. P38 MAPK and intracellular calcium-activated calmodulin-dependent protein kinase IV (CaMKIV) and calcineurin A (CnA) activate transcription of PGC-1, while Akt causes cytoplasmic sequestration of a transcription factor leading to decreased levels of PGC-1.[31] As a cofactor of PPARγ that induces UCP-1 expression, PGC-1 is believed to have a key role in metabolic regulation of WAT to BAT trans-differentiation. In our study, treatment of adipocytes derived from TAO and healthy control patients with bimatoprost showed upregulation of MAPK/ERK, PI3K/Akt, and p38 MAPK phosphorylation products (Fig. 4A). Mechanistic experiments also demonstrated that pharmacologic inhibition of each of these pathways rescues the inhibitory effect of bimatoprost on adipogenesis (Figs. 4B–D). Lastly, the downstream signaling of prostanoid FP receptor via the GPCR-mediated intracellular calcium pathway was demonstrated with a significant increase in calcium transients upon bimatoprost treatment, highlighting the multifaceted and complex signaling pathways engaged. Together, these pathways allowed us to begin to construct the map of the various connections between PG analogues, adipogenesis, and WAT and BAT physiology. Figure 6 demonstrates a proposed working model for the effect of bimatoprost via the combined signaling pathways.

The therapeutic potential of PG analogues in TAO, however, ultimately depends on the clinical applicability and safety in vivo. While bimatoprost already is an approved therapy on the market for elevated IOP, the appropriate mode of delivery, concentration, and dosing for an orbital indication remain unknown. One study of retrobulbar injection of bimatoprost in three rats reported no evidence of inflammation, but increased adipocyte density and heterogeneity.[38] In our study, the same volume and concentration of bimatoprost (100 μL 0.03% bimatoprost) was injected into 8 mouse orbits with pre- and post-injection OCT and PERG, followed by exenteration and histologic examination of the orbital contents. Similar to the previous rat study, there was no evidence of inflammation within the orbital fat compartments. We also showed, for the first time to our knowledge, that there were no detectable

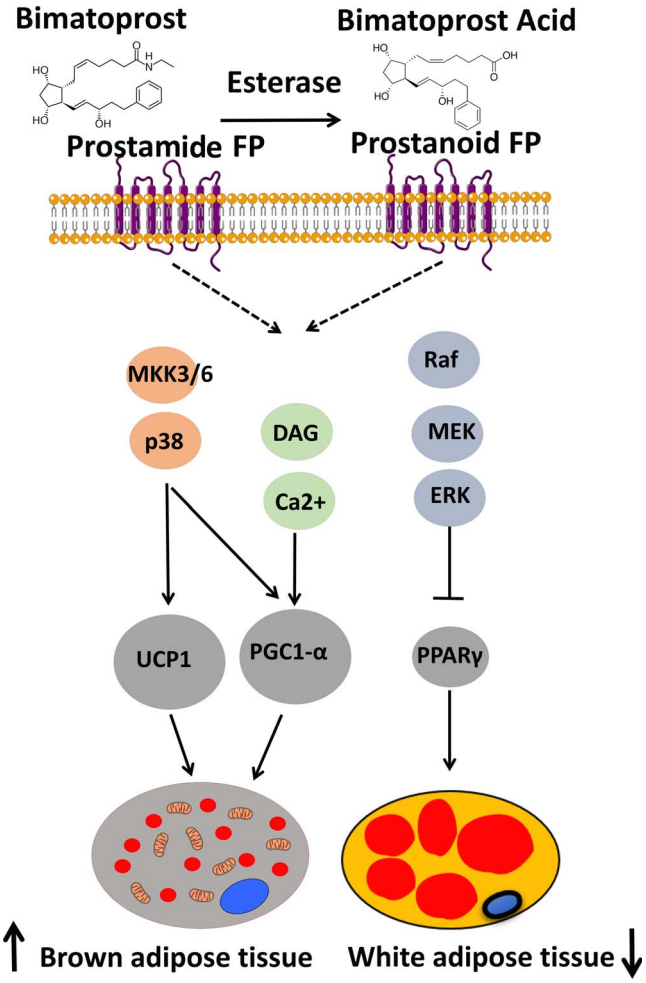

Figure 6. Working model for the mechanism of action: bimatoprost (via bimatoprost acid) can bind to the prostanoid FP receptor, which is a cell surface G-protein-coupled receptor (GPCR), and initiates its intracellular signaling cascades including MAPK, PI3/Akt, p38 MAPK and calcium signaling pathways. Together, these pathways are thought to lead to mitochondrial biogenesis and a thermogenic switch from white to brown adipose tissue.

adverse effects using in vivo imaging and functional studies. Of note, the 0.03% bimatoprost solution available commercially has the micromolar equivalence of 722 μM. This concentration is, in fact, far higher than 1 μM bimatoprost used in our in vitro assays, which was chosen in light of higher concentrations (2 and 10 μM) negatively affecting cell viability in vitro. While the true therapeutic concentration in vivo and in vitro cannot be directly compared, it is encouraging that an injection of 722 μM solution of bimatoprost did not result in detectable toxicity. Although additional in vivo studies are needed to determine the safest and the most effective method of delivery of PG analogues in TAO, our results provide an important starting point.

There are several limitations in the current study. One major limitation in using the in vitro model of OASCs is that the cell culture system is devoid of immune components. Therefore, the cell culture may not faithfully recapitulate the inflammatory milieu of active TAO and the immune responses involved in the pathophysiology of TAO. Secondly, the sample size is small, with only three cell lines each of type 1 TAO and control patients and four cell lines of Type 2 TAO. Further stratification by history of orbital radiation or long-term systemic steroid or

immunomodulator use also would be of interest. Lastly, the use of mouse orbit as a model for intraorbital pathology is limited by the inherent anatomic differences, such as the presence of a large Harderian gland in mice in lieu of retrobulbar fat.

In conclusion, the unexpected point of intersection between TAO and PAP brings forth an interesting clinical question and a potential for a new therapeutic approach to TAO. Using a commercially available PG analogue, bimatoprost, we demonstrated a significant decrease in the cell migration and adipogenic capacity of OASCs derived from TAO patients, and that these effects manifest via a combination of white-to-brown fat trans-differentiation and a number of established intracellular signaling pathways. Results from retrobulbar injection of bimatoprost in mice provide important preliminary building blocks for development of effective PG analogue-derived orbital therapy for TAO. Therefore, our results provided additional insight into the physiology of orbital adipose tissue in controls and TAO and laid the groundwork for potential next steps in translational studies to treat TAO.

Acknowledgments

The authors thank David Tse, MD, FACS, for his mentoship and support of this study. Supported by National Institutes of Health Center Core Grant P30EY014801, Research to Prevent Blindness Unrestricted Grant, Inc. (New York, NY, USA) and the Dr. Nasser Ibrahim Al-Rashid Orbital Vision Research Fund.

Disclosure: **C.J. Choi**, None; **W. Tao**, None; **R. Doddapaneni**, None; **Z. Acosta-Torres**, None; **N.W. Blessing**, None; **B.W. Lee**, None; **D. Pelaez**, None; **S.T. Wester**, None

References

1. Bahn RS. Graves' ophthalmopathy. *N Engl J Med*. 2010;362:726–738.
2. Weetman AP. Graves' disease. *N Engl J Med*. 2000;343:1236–1248.
3. Hiromatsu Y, Yang D, Bednarczuk T, Miyake I, Nonaka K, Inoue Y. Cytokine profiles in eye muscle tissue and orbital fat tissue from patients with thyroid-associated ophthalmopathy. *J Clin Endocrinol Metab*. 2000;85:1194–1199.
4. Garrity JA, Bahn RS. Pathogenesis of graves ophthalmopathy: implications for prediction, prevention, and treatment. *Am J Ophthalmol*. 2006;142:147–153.
5. Kozdon K, Fitchett C, Rose GE, Ezra DG, Bailly M. Mesenchymal stem cell-like properties of orbital fibroblasts in graves' orbitopathy. *Invest Ophthalmol Vis Sci*. 2015;56:5743–5750.
6. Koumas L, Smith TJ, Feldon S, Blumberg N, Phipps RP. Thy-1 expression in human fibroblast subsets defines myofibroblastic or lipofibroblastic phenotypes. *Am J Pathol*. 2003;163:1291–1300.
7. Wakelkamp IM, Bakker O, Baldeschi L, Wiersinga WM, Prummel MF. TSH–R expression and cytokine profile in orbital tissue of active vs. inactive Graves' ophthalmopathy patients. *Clin Endocr*. 2003;58:280–287.
8. Tsui S, Naik V, Hoa N, et al. Evidence for an association between thyroid-stimulating hormone and insulin-like growth factor 1 receptors: a tale of two antigens implicated in Graves' disease. *J Immunol*. 2008;181:4397–4405.
9. Rosen ED, MacDougald OA. Adipocyte differentiation from the inside out. *Nat Rev Mol Cell Biol*. 2006;7:885–896.
10. Smith TJ, Kahaly GJ, Ezra DG, et al. Teprotumumab for thyroid-associated ophthalmopathy. *N Engl J Med*. 2017;376:1748–1761.
11. Liang Y, Woodward DF, Guzman VM, et al. Identification and pharmacological characterization of the prostaglandin FP receptor and FP receptor variant complexes. *Br J Pharmacol*. 2008;154:1079–1093.
12. Maxey KM, Johnson JL, LaBrecque J. The hydrolysis of bimatoprost in corneal tissue generates a potent prostanoid FP receptor agonist. *Surv Ophthalmol*. 2002;47(suppl 1):S34–S40.
13. Taketani Y, Yamagishi R, Fujishiro T, Igarashi M, Sakata R, Aihara M. Activation of the prostanoid FP receptor inhibits adipogenesis leading to deepening of the upper eyelid sulcus in prostaglandin-associated periorbitopathy. *Invest Ophthalmol Vis Sci*. 2014;55:1269–1276.
14. Kucukevcilioglu M, Bayer A, Uysal Y, Altinsoy HI. Prostaglandin associated periorbitopathy in patients using bimatoprost, latanoprost and travoprost. *Clin Exp Ophthalmol*. 2014;42:126–131.
15. Park J, Cho HK, Moon JI. Changes to upper eyelid orbital fat from use of topical bimatoprost, travoprost, and latanoprost. *Jpn J Ophthalmol*. 2011;55:22–27.
16. Choi HY, Lee JE, Lee JW, Park HJ, Lee JE, Jung JH. In vitro study of antiadipogenic profile of latanoprost, travoprost, bimatoprost, and tafluprost in human orbital preadiopocytes. *J Ocul Pharmacol Ther*. 2012;28:146–152.
17. Draman MS, Grennan-Jones F, Zhang L, et al. Effects of prostaglandin F(2alpha) on adipocyte biology relevant to graves' orbitopathy. *Thyroid*. 2013;23:1600–1608.
18. Madsen L, Pedersen LM, Lillefosse HH, et al. UCP1 induction during recruitment of brown adipocytes in white adipose tissue is dependent on cyclooxygenase activity. *PLoS One*. 2010;5:e11391.
19. Lowell BB, Flier JS. Brown adipose tissue, beta 3-adrenergic receptors, and obesity. *Annu Rev Med*. 1997;48:307–316.
20. Johnson KT, Wiesweg B, Schott M, et al. Examination of orbital tissues in murine models of Graves' disease reveals expression of UCP-1 and the TSHR in retrobulbar adipose tissues. *Horm Metab Res*. 2013;45:401–407.
21. Schluter A, Horstmann M, Diaz-Cano S, et al. Genetic immunization with mouse thyrotrophin hormone receptor plasmid breaks self-tolerance for a murine model of autoimmune thyroid disease and Graves' orbitopathy. *Clini Exp Immunol*. 2018;191:255–267.
22. Korn BS, Kikkawa DO, Hicok KC. Identification and characterization of adult stem cells from human orbital adipose tissue. *Ophthal Plast Reconstr Surg*. 2009;25:27–32.
23. Chen SY, Mahabole M, Horesh E, Wester S, Goldberg JL, Tseng SC. Isolation and characterization of mesenchymal progenitor cells from human orbital adipose tissue. *Invest Ophthalmol Vis Sci*. 2014;55:4842–4852.
24. Tao W, Ayala-Haedo JA, Field MG, Pelaez D, Wester ST. RNA-sequencing gene expression profiling of orbital adipose-derived stem cell population implicate HOX genes and WNT signaling dysregulation in the pathogenesis of thyroid-associated orbitopathy. *Invest Ophthalmol Vis Sci*. 2017;58:6146–6158.
25. Wiersinga WM, Bartalena L. Epidemiology and prevention of Graves' ophthalmopathy. *Thyroid*. 2002;12:855–860.
26. Valyasevi RW, Erickson DZ, Harteneck DA, et al. Differentiation of human orbital preadipocyte fibroblasts induces expression of functional thyrotropin receptor. *J Clin Endocr Metab*. 1999;84:2557–2562.
27. Cheng AM, Yin HY, Chen A, et al. Celecoxib and pioglitazone as potential therapeutics for regulating TGF-beta-induced hyaluronan in dysthyroid myopathy. *Invest Ophthalmol Vis Sci*. 2016;57:1951–1959.
28. Ferrari SM, Fallahi P, Vita R, Antonelli A, Benvenga S. Peroxisome proliferator-activated receptor-gamma in thyroid autoimmunity. *PPAR Res*. 2015;2015:232818.
29. Mimura LY, Villares SM, Monteiro ML, Guazzelli IC, Bloise W. Peroxisome proliferator-activated receptor-gamma gene ex-

pression in orbital adipose/connective tissues is increased during the active stage of Graves' ophthalmopathy. *Thyroid*. 2003;13:845–850.

30. Filippopoulos T, Paula JS, Torun N, Hatton MP, Pasquale LR, Grosskreutz CL. Periorbital changes associated with topical bimatoprost. *Ophthal Plast Reconstr Surg*. 2008;24:302–307.
31. Silvestri C, Martella A, Poloso NJ, et al. Anandamide-derived prostamide F2alpha negatively regulates adipogenesis. *J Biol Chem*. 2013;288:23307–23321.
32. Casimir DA, Miller CW, Ntambi JM. Preadipocyte differentiation blocked by prostaglandin stimulation of prostanoid FP2 receptor in murine 3T3-L1 cells. *Differentiation*. 1996;60: 203–210.
33. Serrero G, Lepak NM, Goodrich SP. Prostaglandin F2 alpha inhibits the differentiation of adipocyte precursors in primary culture. *Biochem Biophys Res Commun*. 1992;183:438–442.
34. Smorlesi A, Frontini A, Giordano A, Cinti S. The adipose organ: white-brown adipocyte plasticity and metabolic inflammation. *Obesity Rev*. 2012;13(suppl 2):83–96.
35. Camp HS, Tafuri SR. Regulation of peroxisome proliferator-activated receptor gamma activity by mitogen-activated protein kinase. *J Biol Chem*. 1997;272:10811–10816.
36. Bost F, Aouadi M, Caron L, et al. The extracellular signal-regulated kinase isoform ERK1 is specifically required for in vitro and in vivo adipogenesis. *Diabetes*. 2005;54:402–411.
37. Ho IC, Kim JH, Rooney JW, Spiegelman BM, Glimcher LH. A potential role for the nuclear factor of activated T cells family of transcriptional regulatory proteins in adipogenesis. *Proc Natl Acad Sci U S A*. 1998;95:15537–15541.
38. Eftekhari K, Vagefi MR, Lee V, et al. In vivo effects of retrobulbar bimatoprost injection on orbital fat. *Ophthal Plast Reconstr Surg*. 2018;34:201–204.

Investigative Ophthalmology & Visual Science